where A is the relevant presented area of the reciprocating element. Equation (3.94) thus gives the damping due to gas spring hysteresis. All the relevant linear equations are listed in table 3.3.

Table 3.3 Set of linearised equations for pressure, pressure drop and gas spring hysteresis damping.

Compression space pressure	$p_c \simeq p_{mean}\left(1 - \dfrac{A_D(x_d + x_c)}{T_h S} - \dfrac{A_P x_p - (A_D - A_R)x_d}{T_k S}\right)$
	where
	$S = \dfrac{A_P C_C}{T_k} + \dfrac{V_k}{T_k} + \dfrac{V_r \ln(T_h/T_k)}{(T_h - T_k)} + \dfrac{V_h}{T_h} + \dfrac{A_D E_E}{T_h}$
Pressure drop	$A_D \Delta_p = C_p \dot{x}_p + C_d \dot{x}_d + C_c \dot{x}_c$
	where
	$C_p = A_P A_D P_C \quad C_d = -(2A_D - A_R)A_D P_C \quad C_c = -A_D{}^2 P_C$
	and
	$P_C = \frac{4}{3}(1/\pi)[\rho_k U_k (f_t + k_h)_k / A_k + \rho_h U_h (f_t + k_h)_h / A_h] + f_l / A_r$
Gas spring hysteresis damping	$C_H = \dfrac{k}{2}\sqrt{\dfrac{\omega}{2\alpha_0}}\gamma(\gamma - 1)T_w A_w \left(\dfrac{A}{\omega V_B}\right)^2$

Note that other methods may be used to generate the linear functions. For example, if a sophisticated computer simulation is used to analyse the thermodynamic cycle, the pressure variations will only be known implicitly. In this case, volume variations would be assumed, the resulting pressure variations analysed by Fourier techniques and then, using only the linear terms, the dynamic analysis would be performed to obtain new volume variations. This process is therefore iterative unless one is solving for the reciprocating masses, in which case the solution is obtained directly. The second-order terms neglected should be of the order of 10% or less of the linear terms (Gedeon 1978). Particular examples are now considered.

3.4 The Sunpower RE-1000 engine

The RE-1000 was developed at Sunpower to investigate free-piston Stirling engine applications. The engine is primarily a research machine and is the seventh in a series which began with an engine being built for the American Gas Association (Beale *et al* 1975). The power to load is of the order of 1 kW (figure 3.7).

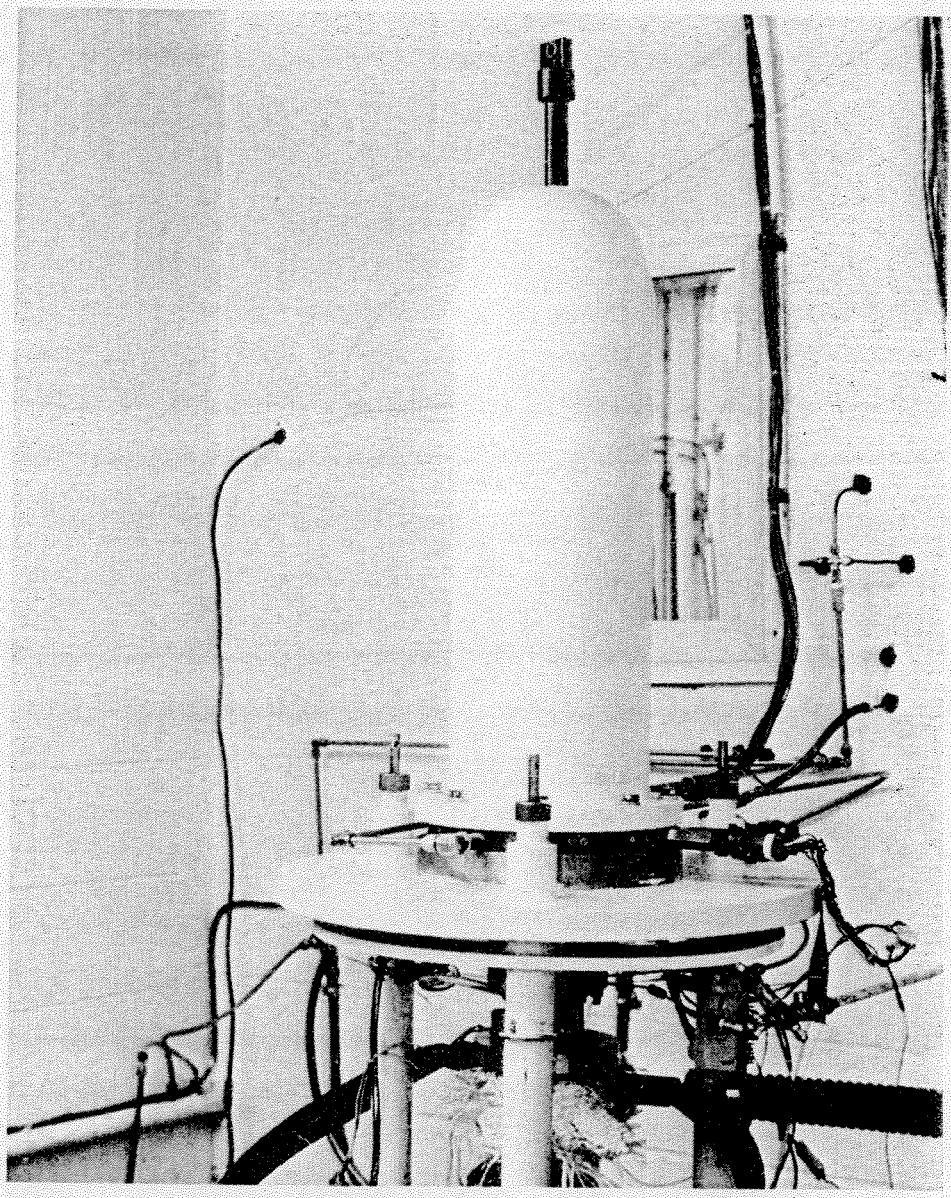

Figure 3.7 Sunpower RE-1000 engine (courtesy Sunpower Incorporated).

Referring to figure 3.8(*a*), the equations of motion are

$$M_P\ddot{x}_p = A_P(p_c - p_b) - (C_{pc} + C_{H_{pc}})(\dot{x}_p + \dot{x}_c) \tag{3.95}$$

$$M_D\ddot{x}_d = A_D\Delta_p + A_R(p_c - p_d) - C_{H_{dc}}(\dot{x}_d + \dot{x}_c) \tag{3.96}$$

$$M_C\ddot{x}_c = A_D(p_c + \Delta_p - p_b) + A_R(p_c - p_d) - (C_{pc} + C_{H_{pc}})(\dot{x}_c + \dot{x}_p) - K_C x_c \tag{3.97}$$

where the expansion space pressure is taken to be given by

$$p_e = p_c + \Delta_p.$$

This engine has two active gas springs. The pressure variations for these spaces are:

$$p_b = p_{mean}\{V_B/[V_B - A_P(x_p + x_c)]\}^{\gamma} \tag{3.98}$$

$$p_d = p_{mean}\{V_D/[V_D - A_R(x_d + x_c)]\}^{\gamma}. \tag{3.99}$$

Linearising equations (3.98) and (3.99) by the same method that is used for the working gas pressure, the following are obtained:

$$p_b \simeq p_{mean}[1 + \gamma(A_P/V_B)(x_p + x_c)] \tag{3.100}$$

$$p_d \simeq p_{mean}[1 + \gamma(A_R/V_D)(x_d + x_c)]. \tag{3.101}$$

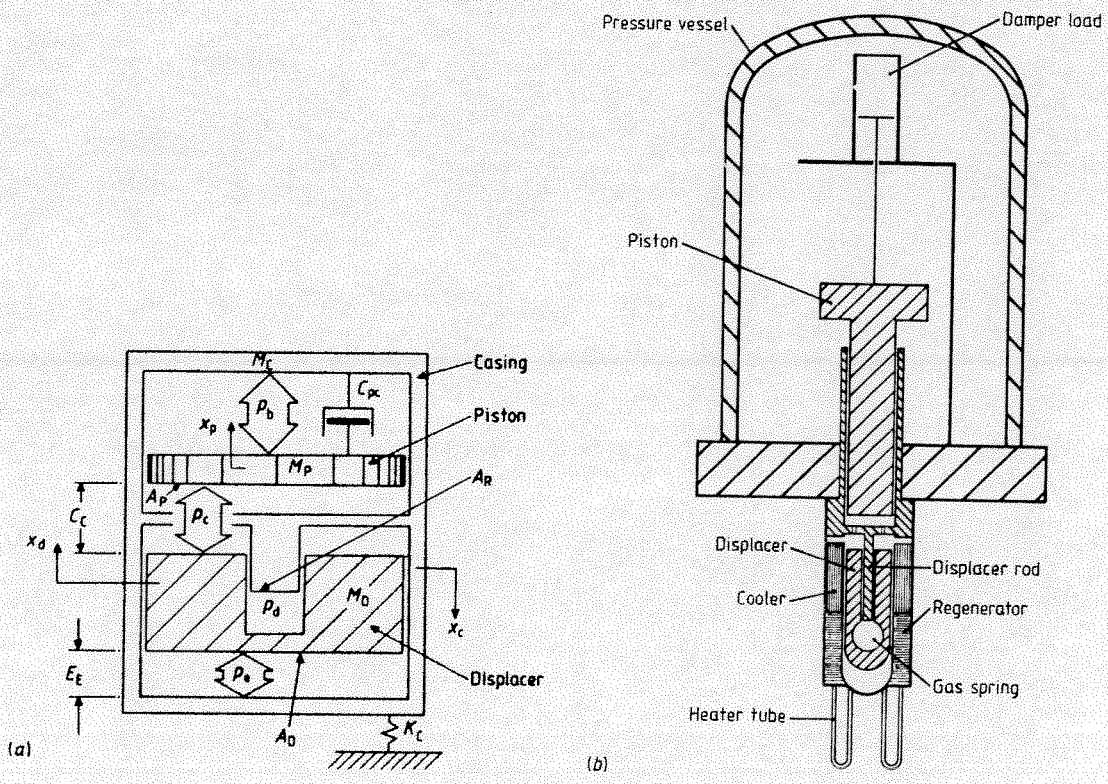

Figure 3.8 Sunpower RE-1000 engine: (*a*) Notation; (*b*) Schematic.

Equations (3.100) and (3.101), together with the linearised equations from table 3.3 are substituted into the equations of motion (3.95), (3.96) and (3.97). Since this is a piston motion mode engine the terms due to the casing motion may be neglected. The casing spring term (S_{cc}), though, is required to ensure that the condition for small casing motions is met. The remaining linear coefficients follow directly by inspection. They are:

$$S_{pp} = -\frac{A_P^2}{M_P}p_{mean}\left(\frac{1}{T_k S} + \frac{\gamma}{V_B}\right) \qquad S_{pd} = -\frac{A_P^2}{M_P S}p_{mean}\left(\frac{1}{T_h} - \frac{(1 - A_R/A_P)}{T_k}\right)$$

$$D_{pp} = -(C_{pc} + C_{H_{pc}})/M_P \qquad D_{pd} = 0$$

$$S_{dp} = -\frac{A_P A_R p_{mean}}{M_D T_k S} \qquad S_{dd} = -\frac{A_R}{M_D} p_{mean}\left(\frac{A_P}{T_h S} - \frac{(A_P - A_R)}{T_k S} + \gamma \frac{A_R}{V_D}\right)$$

$$D_{dp} = C_p / M_D \qquad D_{dd} = (C_d - C_{H_{dc}})/M_D$$

$$S_{cc} = -\frac{A_P{}^2}{M_C} p_{mean}\left(\frac{1}{T_h S} + \frac{\gamma}{V_B} + \frac{A_R/A_P}{T_h S} + \frac{\gamma (A_R/A_P)^2}{V_D}\right) - \frac{K_C}{M_C}.$$

For this particular configuration note that $A_P = A_D$.

From table 3.1 (setting $D_{pd} = 0$) the set of dynamic equations for this configuration becomes:

frequency

$$\omega^2 = (D_{dp} S_{pd} - D_{dd} S_{pp} - S_{dd} D_{pp})/(D_{dd} + D_{pp}) \tag{3.102}$$

geometric constraint

$$\omega^4 + \omega^2 (S_{pp} + S_{dd} - D_{dd} D_{pp}) + S_{dd} S_{pp} - S_{dp} S_{pd} = 0 \tag{3.103}$$

piston–displacer phase angle

$$\phi = \tan^{-1}\left(\frac{\omega D_{pp}}{-(S_{pp} + \omega^2)}\right) \tag{3.104}$$

piston–displacer amplitude ratio

$$\frac{X_d}{X_p} = r = \frac{(\omega^2 + S_{pp})^2 + \omega^2 D_{pp}{}^2}{S_{pd}[(\omega^2 + S_{pp})^2 + \omega^2 D_{pp}{}^2]^{1/2}}. \tag{3.105}$$

From the frequency equation, it can be seen that since the load coefficient D_{pp} appears in this equation, these machines will in general have a load-dependent frequency. However, by careful choice of the geometric parameters, it is possible to alter this characteristic and achieve almost constant frequency for a wide range of loads. Obviously, there are many applications where this might be desirable. It is instructive to see how this engine can be designed for constant frequency operation.

On all free-piston machines the displacer is typically much lighter than the piston, thus

$$D_{dd} \gg D_{pp} \tag{3.106}$$

and by arranging that

$$|D_{dd} S_{pp}| \gg |D_{dp} S_{pd} - S_{dd} D_{pp}| \tag{3.107}$$

equation (3.102) becomes

$$\omega^2 = -S_{pp} \tag{3.108}$$

which is independent of the load and gives the operating frequency as simply the natural frequency of the piston.

The geometric constraint equation must also be satisfied. This may be done in various ways, one of which is to arrange the following:

$$S_{dd} = D_{dd} D_{pp} \tag{3.109}$$

and

$$S_{dd} S_{pp} = S_{dp} S_{pd}, \tag{3.110}$$

thus reducing equation (3.103) to the same result as that expressed by (3.108). Equations (3.106), (3.107), (3.109) and (3.110) specify how the geometry must be arranged to achieve constant frequency operation.

The phase angle under these conditions is also constant:

$$\phi = -90°. \tag{3.111}$$

The amplitude ratio is, however, load† dependent

$$r = \omega D_{pp} / S_{pd} \tag{3.112}$$

which results in a load dependent power.

Note that for constant frequency operation the piston and the displacer are in quadrature, and consequently the optimum phase angle will not in general be satisfied. Thus, when designing this engine for constant frequency operation, there is often a trade-off on available power. On the other hand, if the machine is not designed for constant frequency operation, its capacity to tolerate load variation is much reduced, and such machines tend to operate best as fixed load devices.

The RE-1000 was not specifically designed as a constant frequency device. However, it does operate at essentially constant frequency over a nominal change in load. The design point operating conditions and geometric data are listed in table 3.4. Table 3.5 compares the dynamic operating parameters predicted by the linear analysis with those of a complete simulation and also with experimental values. The agreement can be seen to be good, which indicates that this rather simple analysis can return realistic results. The geometric constraint equation was used only to calculate the bounce space volume V_B.

It is usually important to know how frequency and power will vary with the load damping. This may be done by plotting the frequency and power as a function of D_{pp}. However, to do this presents somewhat of a difficulty, since the geometric constraint equation would typically only be satisfied for a particular value of D_{pp}. In a real machine, what happens is that as the amplitudes and frequency change in response to a load change, the viscous damping in the heat exchangers also changes (approximately proportional to velocity to the 1.75 power). Thus, in a well designed machine the viscous

†The term *load* may be confusing here: the load is the damper to which the engine dissipates its power.

Table 3.4 Sunpower RE-1000 Engine data.

General	
Working fluid	Helium
Mean pressure	$p_{mean} = 71$ bar
Mean hot space temperature	$T_h = 814.3$ K
Mean cold space temperature	$T_k = 322.8$ K
Geometric	
Cooler volume	$V_k = 20.43\ cm^3$
Regenerator volume	$V_r = 56.37\ cm^3$
Heater volume	$V_h = 27.33\ cm^3$
Displacer rod area	$A_R = 2.176\ cm^2$
Piston frontal area	$A_P = 25.69\ cm^2$
Displacer spring volume	$V_D = 37.97\ cm^3$
Piston bounce space volume	$V_B = 2615.0\ cm^3$
Expansion space clearance	$E_E = 18.61$ mm
Compression space clearance	$C_C = 18.30$ mm
Masses	
Piston	$M_P = 6.20$ kg
Displacer	$M_D = 0.426$ kg
Casing	$M_C = 416.0$ kg
Dynamic	
Heat exchanger pressure drop and phase with respect to piston	0.5 bar at 166.4°
Piston amplitude	$X_p = 11.45$ mm
Displacer amplitude	$X_d = 12.33$ mm
Load damping	$C_{pc} = 461.5\ Ns\ m^{-1}$
Displacer gas spring damping	$C_{H_{dc}} = 35.34\ Ns\ m^{-1}$

damping tends to stabilise the motions. To model this effect with the linear analysis it is assumed that D_{dd} and D_{dp} change to effect closure, i.e. that the geometric constraint equation is simultaneously satisfied by allowing D_{dd} and D_{dp} to change. For the RE-1000 the D_{dp} term makes a negligible contribution to the frequency and power calculations and is neglected. Therefore the frequency equation and the geometric constraint equation are simultaneously satisfied by allowing only D_{pp} to vary. The performance characteristics so determined are shown in figure 3.9. It can be seen that for a load change of 100 %, the change in frequency is only 13 %. The power, though, changes quite dramatically.

The power calculation assumes that the piston amplitude remains constant and that the displacer amplitude varies according to the amplitude ratio equation. In reality, both the displacer and the piston change their amplitudes in response to a load change, the ratio of these two amplitudes being given by

Table 3.5 Linear analysis results and comparison with simulation and experiment (RE-1000 engine)

Linear coefficients

$S_{pp} = -5.345 \times 10^4$
$S_{pd} = 2.983 \times 10^4$
$D_{pp} = -74.44$
$S_{dp} = -7.086 \times 10^4$
$S_{dd} = 2.121 \times 10^3$
$D_{dp} = 70.82$
$D_{dd} = -506.4$
$S_{cc} = -547.7$

	Linear analysis	Simulation	Experiment
Frequency (Hz)	33.2	30.0	30.0
Phase angle (°)	−57.9	−43.7	−42.5
Amplitude ratio	0.62	1.08	1.06
Output power (based X_p) (kW)	1.32	1.08	1.00
Output power (based X_d)	2.00	—	—

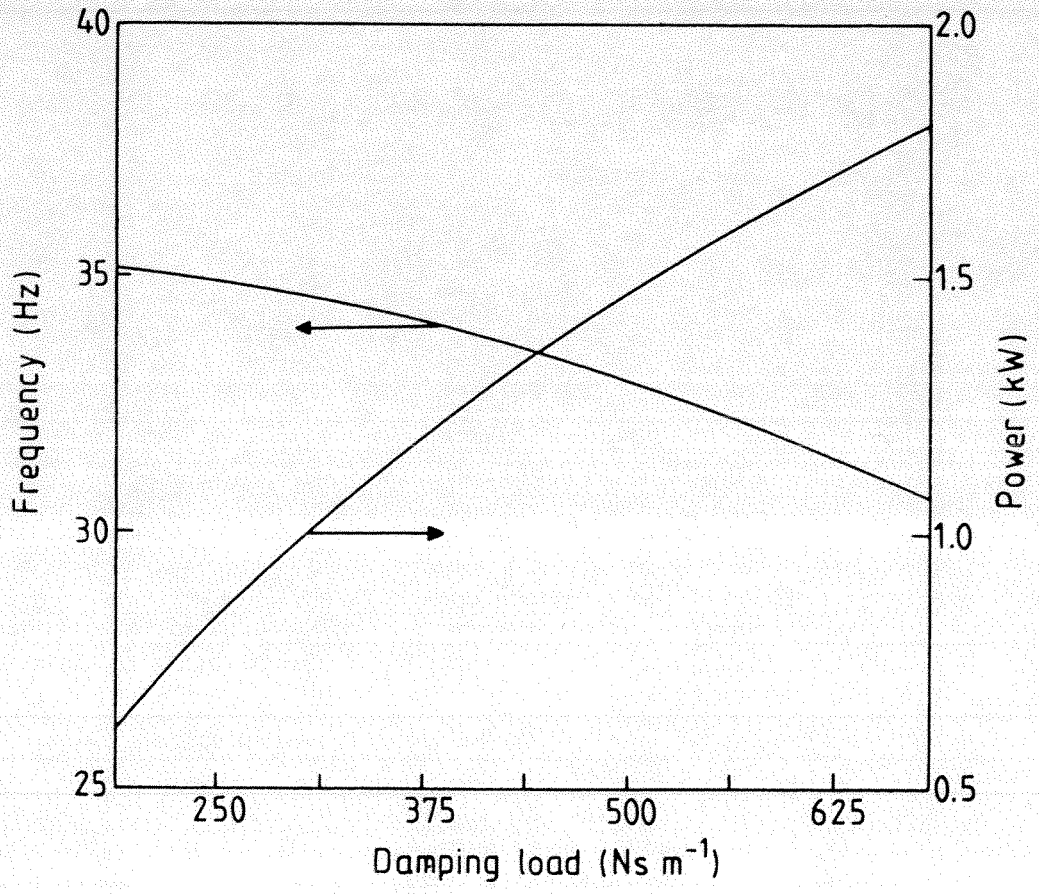

Figure 3.9 Frequency and power versus load for the Sunpower RE-1000 engine.

the amplitude ratio equation. A more accurate way of assessing the power curve is to ensure that the thermodynamic pV power and the power dissipated in the load are approximately equal, by solving for the piston amplitude that will make this so.

3.5 The Sunpower M100 free-cylinder engine

This machine is an example of a casing mode engine developed at Sunpower which has proved to be a very reliable performer (See Beale (1979) and Beale *et al* (1971), and also figure 3.10). The engine is used to drive a water pump by the action of its cylinder. In this form it has been extensively tested both in the field and laboratory. One of the most attractive features of this engine is that it is constructed from inexpensive easy-to-obtain components. In fact, the entire pump housing is fabricated from ordinary PVC piping and fixtures that may be purchased at any reasonably equiped hardware shop. The reliability, simplicity and low cost of this engine make it an eminently suitable device for application in developing countries.

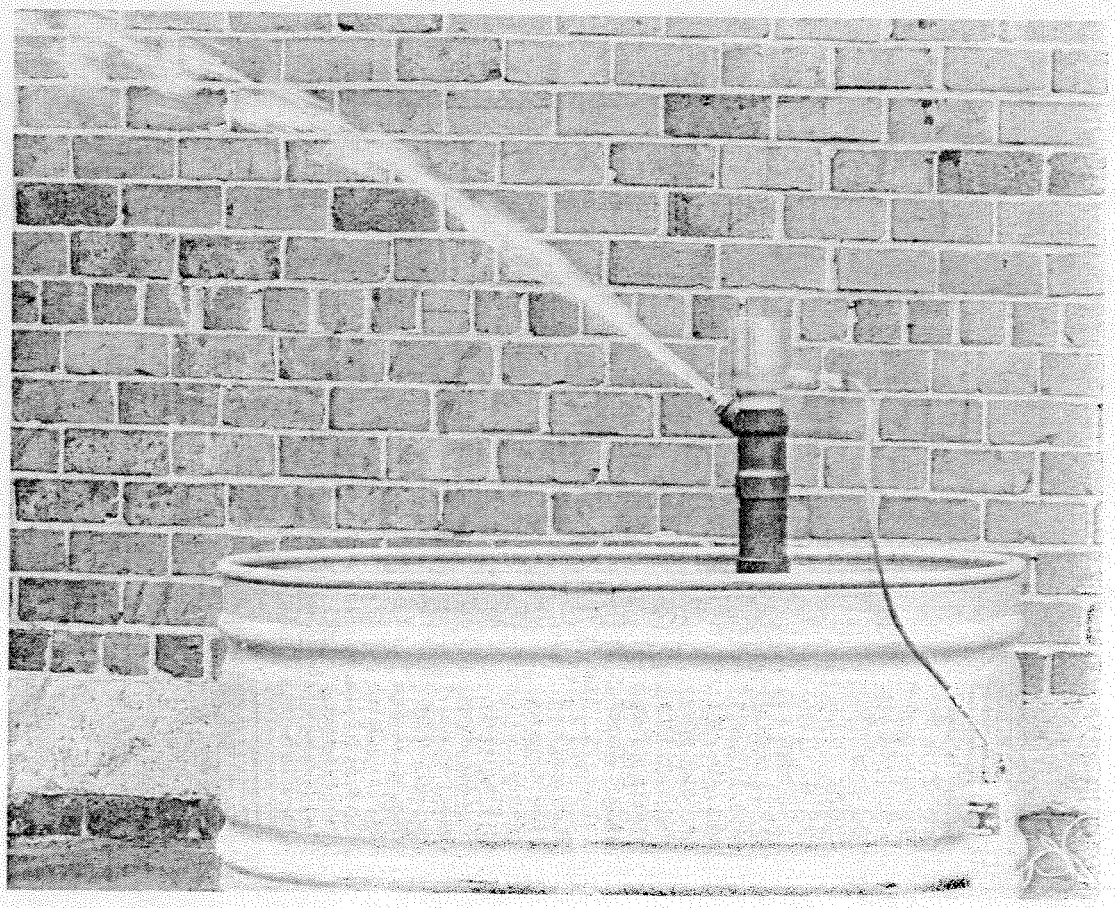

Figure 3.10 Sunpower M100 free-cylinder engine (courtesy Sunpower Incorporated).

Referring to figure 3.11(*a*), the equations of motion for this engine are

$$M_P\ddot{x}_p = A_R p_d + A_P p_c - A_D p_b \tag{3.113}$$

$$M_D\ddot{x}_d = A_R(p_c - p_d) + A_D\Delta p - C_{H_{dp}}(\dot{x}_d - \dot{x}_p) \tag{3.114}$$

$$M_C\ddot{x}_c = A_D(p_c + \Delta p - p_b) - C_L\dot{x}_c \tag{3.115}$$

where positive directions are taken as those which increase the working gas volume and it is assumed that the load may be represented by a damper acting on the casing C_L.

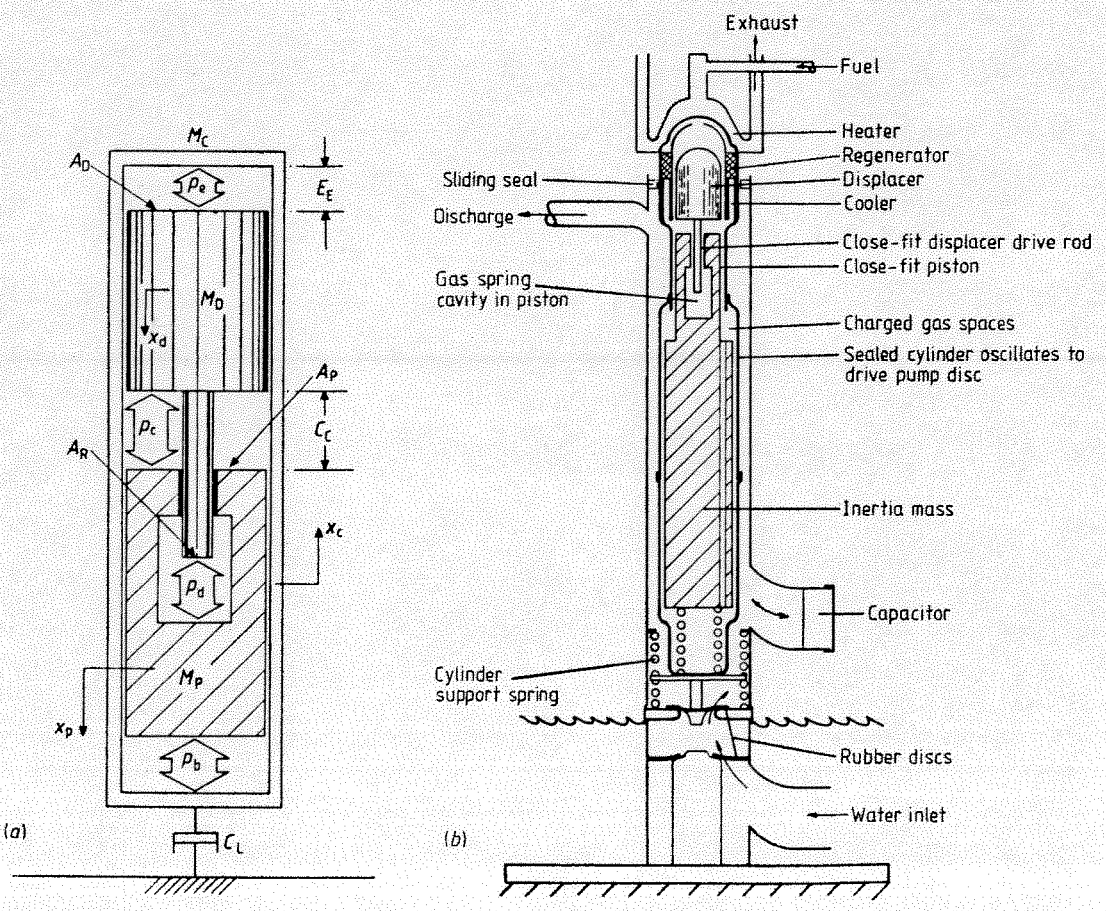

Figure 3.11 Sunpower M100 free-cylinder engine: (*a*) Notation; (*b*) Schematic. NB: The support springs are usually weak compared with the gas springs and make no significant contribution to the spring forces. They have therefore been neglected in the analysis.

This engine has only one active gas spring, the displacer gas spring. The pressure variation for this space is given by

$$p_d = p_{mean}\{V_D/[V_D - A_R(x_d - x_p)]\}^\gamma, \tag{3.116}$$

which is linearised to

$$p_d \simeq p_{mean}\,[1+\gamma(A_R/V_D)(x_d - x_p)]. \tag{3.117}$$

Owing to the large bounce space volume the pressure variation in this space is small and may be safely neglected. Thus

$$p_b \simeq p_{mean}. \tag{3.118}$$

Since this is a casing motion engine it is possible to neglect the motions of the piston if its natural frequency is small compared with the operating frequency. By substituting the linearised equations into the equations of motion, the relevant linear coefficients follow by inspection:

$$S_{pp} = -\frac{p_{mean}}{M_P}\left(\frac{A_P^2}{T_k S} + \gamma\frac{A_R^2}{V_D}\right)$$

$$S_{dd} = \frac{A_R}{M_D}p_{mean}\left(\frac{A_P}{T_k S} - \frac{A_D}{T_h S} - \gamma\frac{A_R}{V_D}\right) \qquad S_{dc} = -\frac{A_D A_R p_{mean}}{M_D T_h S}$$

$$D_{dd} = (C_d - C_{H_{dp}})/M_D \qquad D_{dc} = C_c/M_D$$

$$S_{cd} = \frac{A_D}{M_C S}p_{mean}\left(\frac{A_P}{T_k} - \frac{A_D}{T_h}\right) \qquad S_{cc} = -\frac{A_D^2 p_{mean}}{M_C T_h S}$$

$$D_{cd} = C_d/M_C \qquad D_{cc} = (C_c - C_L)/M_C.$$

Unfortunately, for this case it is not possible to simplify the dynamic equations (table 3.1).

Table 3.6 lists the design point operating conditions and geometric data for the engine. A detailed comparison between the experimental and linear results is not possible, since the machine was never fully instrumented. However, the net pumping power, cylinder stroke and frequency were measured. A comparison of these quantities with the linear results is given in table 3.7. Notwithstanding that the pump efficiency is not known, the correlation is excellent on frequency and certainly of similar magnitude on power. In this example, the geometric constraint equation was used to evaluate the displacer gas spring volume V_D.

The performance characteristics as calculated by this analysis are shown in figure 3.12. It is interesting to note that the power change is quite small (18 %) for a considerable change in load (over 100 %). This is very advantageous for certain applications, for example, as an agricultural water pumping machine. In such a situation it could be expected that the pumping load could vary widely.

The cylinder stroke versus load is shown in figure 3.13. It can be seen that at the higher power levels the amplitude is much reduced. The amount of water pumped is, of course, directly proportional to the stroke.

Table 3.6 Sunpower M100 free-cylinder engine data.

General	
Working fluid	Helium
Mean pressure	$p_{mean} = 22$ bar
Mean hot space temperature	$T_h = 866.6$ K
Mean cold space temperature	$T_k = 322.3$ K
Geometric	
Cooler volume	$V_k = 3.41\ cm^3$
Regenerator volume	$V_r = 25.4\ cm^3$
Heater volume	$V_h = 2.42\ cm^3$
Displacer rod area	$A_R = 1.327\ cm^2$
Piston frontal area	$A_P = 7.744\ cm^2$
Displacer frontal area	$A_D = 9.071\ cm^2$
Displacer spring volume	$V_D = 9.95\ cm^3$
Expansion space clearance	$E_E = 20.0$ mm
Compression space clearance	$C_C = 16.0$ mm
Masses	
Piston	$M_P = 10$ kg
Displacer	$M_D = 78.5$ g
Casing	$M_C = 3.3$ kg
Dynamic	
Displacer amplitude	$X_d = 15.0$ mm
Cylinder amplitude	$X_c = 5.0$ to 7.5 mm
Load damping (approximate)	$C_L = 132.0\ Ns\ m^{-1}$
Displacer gas spring damping (approximate)	$C_{H_{dp}} = 2.3\ Ns\ m^{-1}$

Table 3.7 Linear analysis results and comparison with experiment (M100 free-cylinder engine).

Linear coefficients

$S_{pp} = -3.829 \times 10^3$	$S_{cd} = 6.909 \times 10^3$
$S_{dd} = -3.381 \times 10^4$	$S_{cc} = -5.333 \times 10^3$
$S_{dc} = -3.280 \times 10^4$	$D_{cd} = -0.714$
$D_{dd} = -29.95$	$D_{cc} = -40.0$
$D_{dc} = 15.43$	

	Linear analysis	Experiment
Frequency (Hz)	22.4	23.0
Amplitude ratio	2.25	2.5†
Output power (W)	58.5	40.0†

† Approximate values

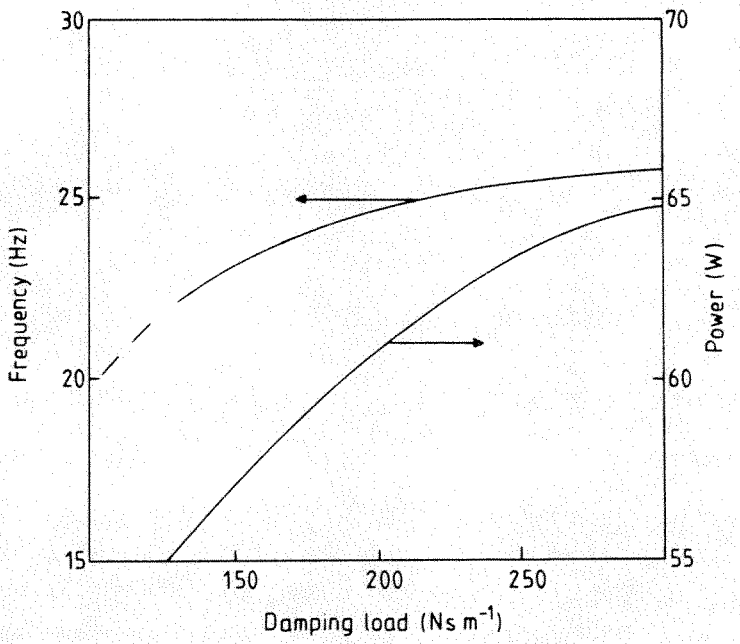

Figure 3.12 Frequency and power versus load for the Sunpower M100 free-cylinder engine.

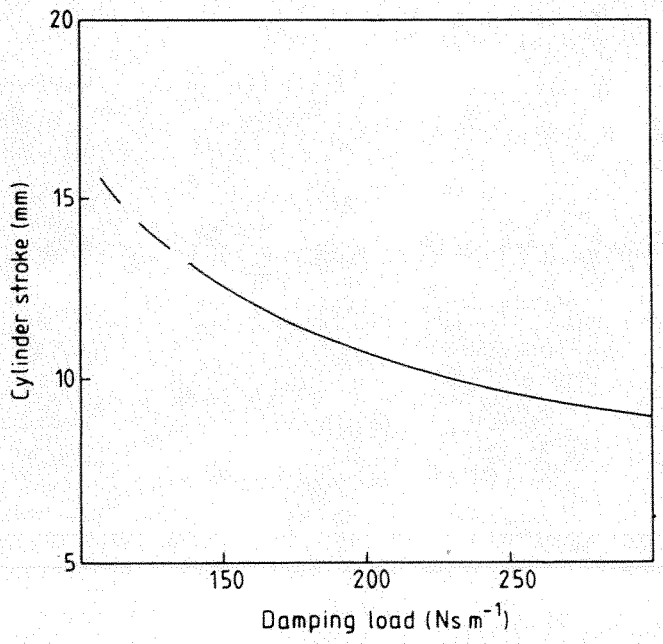

Figure 3.13 Stroke versus load for the Sunpower M100 free-cylinder engine.

3.6 The Harwell Thermo-Mechanical Generator (TMG)

The TMG is a unique free-piston machine in many respects. Instead of a piston, this engine has a diaphragm which flexes to effect the change of working gas volume. In addition, the stiffness of the diaphragm acts as a mechanical spring.